

Bragg spectroscopy of clean and disordered lattice bosons in one dimension: a spectral fingerprint of the Bose glass

Guillaume Roux¹, Anna Minguzzi², and Tommaso Roscilde³

¹ LPTMS, Univ. Paris-Sud, CNRS, UMR8626, F-91405 Orsay, France.

² Université Grenoble-Alpes and CNRS, Laboratoire de Physique et Modélisation, des Milieux Condensés UMR 5493, Maison des Magistères, B.P. 166, 38042 Grenoble, France

³ Laboratoire de Physique, CNRS UMR 5672, Ecole Normale Supérieure de Lyon, Université de Lyon, 46 Allée d'Italie, Lyon, F-69364, France

E-mail: guillaume.roux@u-psud.fr, minguzzi@grenoble.cnrs.fr, tommaso.roskilde@ens-lyon.fr

Abstract. We study the dynamic structure factor of a one-dimensional Bose gas confined in an optical lattice and modeled by the Bose-Hubbard Hamiltonian, using a variety of numerical and analytical approaches. The dynamic structure factor, experimentally measurable by Bragg spectroscopy, is studied in three relevant cases: in the clean regime, featuring either a superfluid or a Mott phase; and in the presence of two types of (quasi-)disordered external potentials: a quasi-periodic potential obtained from a bichromatic superlattice and a box random disorder - both featuring a Bose glass phase. In the clean case, we show the emergence of a gapped doublon mode (corresponding to a repulsively bound state) for incommensurate filling, well separated from the low-energy acoustic mode. In the disordered case, we show that the dynamic structure factor provides a direct insight into the spatial structure of the excitations, unveiling their localized nature, which represents a fundamental signature of the Bose glass phase. Furthermore, it provides a clear fingerprint of the very nature of the localization mechanism which differs for the two kinds of disorder potentials we consider. In special cases, the dynamic structure factor may provide an estimate of the position of the localization transition from superfluid to Bose glass, in a complementary manner to the information deduced from the momentum distribution.

PACS numbers: 03.75.Lm, 61.44.Fw, 67.85.Hj, 71.23.Jk

Submitted to: *New J. Phys.*

1. Introduction

In interacting Bose fluids, the interplay between the effect of disorder and that of strong interactions displays a rich showcase of different behaviours. Ultracold atoms offer remarkably the possibility of exploring such an interplay, since in recent experiments both disorder and interactions are natural tuning knobs [1]. In these systems, disorder is realized either by the application of a speckle potential [2, 3, 4, 5, 6, 7], or by a bichromatic optical lattice composed of two incommensurate standing waves [8, 9, 10, 11, 12, 13, 14, 15], giving rise to a quasi-periodic (QP) potential [16].

In a Bose fluid at zero temperature, Bose-Einstein condensation (or quasi-condensation in one dimension) occurs generically in the absence of disorder and in the weakly interacting limit. We consider two ways of destabilizing this phase on a lattice: either via Mott localization due to strong repulsion at commensurate filling; or via Anderson localization due to strong disorder at any filling [17, 18, 19]. The resulting phases - a Mott insulator for strong repulsion, and a Bose glass for strong disorder (and finite repulsion) - are very different forms of non-condensed Bose fluids. Yet, from the point of view of coherence properties, experimentally probed by time-of-flight measurements in cold-atom setups, the two phases look similar. In both cases phase correlations decay exponentially, giving rise to a broad peak in the momentum distribution. Hence additional information is required for a direct observation of the Bose-glass phase, which has been long sought in the context of Bose fluids.

On the other hand, the Bose glass and the Mott insulator are fundamentally distinguished by the nature of their excitation spectrum. The lowest energy excitation in a Mott insulator is a particle-hole excitation with a gap imposed by the energy cost of the multiple occupation of a lattice site. In the limit of very strong repulsion, suppressing density fluctuations, such an excitation can be seen as a free particle/free hole moving on a static background of particles at integer filling. On the other hand, the lowest excitations in a Bose glass are *gapless*, and associated with phonon-like modes localized in rare, locally homogeneous regions of the sample. Therefore not only the density of states, but the spatial structure of the excitations provides a distinct fingerprint of the Bose glass phase with respect to the Mott insulating one.

In this respect, the dynamic structure factor, probed by Bragg spectroscopy in cold-atom experiments [20], offers the possibility of characterizing both the spectral density of the excitations as well as their localized/delocalized nature.

In the weakly-interacting regime, the dynamic structure factor can be estimated using the Bogoliubov approach [21], while at arbitrary interactions in the 1D uniform system can be obtained from the Bethe-Ansatz solution of the integrable Lieb-Liniger model [22, 23, 24], the long-wavelength behaviour in this regime is also captured by Luttinger liquid theory [25]. In the presence of a lattice, the dynamic structure factor has been the subject of several analytical [26, 27, 28] and numerical [29, 30, 31, 32, 33, 34, 35] studies, as well as of recent experiments [36, 37, 38, 39, 40]. In the presence of a disordered potential, only a few studies have addressed the dynamic response functions

of lattice bosons such as the response for lattice modulation spectroscopy [41] and the single-particle spectral function [42], but we are not aware of previous studies of the dynamic structure factor. In particular the response to lattice modulation spectroscopy is sensitive to energy only, and it lacks the momentum resolution which, as anticipated in [43] from the study of the spatial Fourier spectrum of single-particle excitations, is essential to unveil the localized nature of excitations.

In this paper, we aim at an extensive investigation of the dynamic structure factor in the case of one-dimensional Bose gases in an optical lattices, and for widely different regimes, encompassing the weakly interacting limit, the infinitely repulsive case (Tonks limit), and the regime of intermediate interactions. The two limits of weakly interacting and infinitely repulsive particles lend themselves to very convenient theoretical approaches (via Bogolyubov theory and fermionization, respectively), while the intermediate regime, which is the most challenging, can be investigated via exact diagonalization. We particularly focus our attention on the case of a quasi-periodic potential, featuring a localization transition for a finite potential depth even in the non-interacting limit - and we underline the analogies and fundamental differences with respect to a truly random potential.

Our main result is that the dynamic structure factor serves as a very effective diagnostic tool of the localized phases, and, in selected cases, it might provide a quantitative method to estimate the quantum phase transition from superfluid to Bose glass, based upon the localization of the elementary excitations, and therefore complementary to the analysis of the coherence properties. In particular, the dynamic structure factor provides clear signatures of the underlying localization mechanism at play, in all interacting regimes, and it allows to characterize the Bose-glass phase far beyond its thermodynamic definition as a compressible and insulating phase.

The paper is organized as follows. Section 2 introduces the model under investigation, *i.e.* the one-dimensional Bose-Hubbard model in a (quasi-)disordered potential, and the dynamic structure factor. Section 3 recalls some results on the limiting cases (weak interaction and infinite interaction) of the clean system, and it discusses exact diagonalization results interpolating between these limiting cases. Section 4 studies in details the disordered models: Section 4.1 describes the dynamic structure factor in the case of weakly interacting bosons, treated via a Bogolyubov approach, while Section 4.2 focuses on the exact solution in the case of hardcore bosons; Section 4.3 bridges the two above regimes, contrasting the dynamic structure factor across the localization transition with the same quantity across the Mott transition in the absence of disorder. Section 5 contains a discussion on the relevance to experiments while Section 6 is dedicated to conclusions.

2. Bose-Hubbard Hamiltonians in the presence of disorder and methods

2.1. Models

We describe one-dimensional bosons in a deep lattice potential and subject to an external potential using the Bose-Hubbard Hamiltonian,

$$\mathcal{H} = -J \sum_j [b_{j+1}^\dagger b_j + \text{h.c.}] + \frac{U}{2} \sum_j n_j(n_j - 1) + \sum_j w_j n_j. \quad (1)$$

Here b_j^\dagger is the operator creating a boson at site j , $n_j = b_j^\dagger b_j$ is the local density, J is the hopping amplitude and U is the onsite repulsion. We consider lattices with L sites and N particles, *i.e.* a filling factor $n = N/L$. We denote the lattice spacing by a in the figures – when not appearing explicitly in the equations, it is understood that $a = 1$. The w_j are site-dependent energies which account for both the disorder potential and the possible presence of a harmonic trapping potential. For what concerns the disorder distributions, we will focus on two different forms of (quasi-)disorder:

- (i) A quasi-periodic (QP) potential obtained via a bichromatic optical lattice [8], with the form

$$w_j = \frac{V}{2} \sum_j [1 + \cos(2r\pi j + 2\phi)] \quad (2)$$

with r an irrational number and ϕ a random phase-shift on which averaging can be performed. We choose the experimentally relevant value $r = 830/1076$ [9]; when considering periodic boundary conditions on a lattice of size L , we take r as the best rational approximant in the form M/L (where M is a positive integer), so that the potential describes a single period over the entire lattice.

- (ii) A random-box (RB) disorder, for which w_j is a random variable uniformly distributed over the interval $[0, V]$.

In both cases, V/J gives the relative strength of the (quasi-)disorder potential, and it is chosen in such a way that, in the atomic limit, the (quasi-)disorder closes the Mott gap for $V = U$. The main difference among the two types of disorder is that, in the absence of interactions, the QP potential leads to localization of the single-particle wavefunctions above a critical disorder threshold $V = 4J$ [16] while for the RB disorder localization occurs at an infinitesimal disorder strength. The RB phase diagram was studied numerically in Refs. [44, 45, 46, 47, 48]. In the case of the QP potential, the localization mechanism and the features of the single-particle wavefunctions and spectrum was extensively studied [16, 49, 50, 51, 52, 53, 54]. In particular, a simple interpretation can be given in terms of successive band-folding processes (see e.g. Ref. [51, 55, 43]) or at a semi-classical level [51, 56]. Bosonization studies [57, 58] also show that the quasi-periodic potential is different from the pure disorder one, in particular, it does not share the same expected universal Luttinger parameter value at the localization transition, which was checked in Ref. [43]. The phase diagram of the bichromatic system was investigated numerically in Refs. [59, 60, 43, 61].

2.2. Dynamic structure factor

The dynamic structure factor $S(k, \omega)$ is given by the space-time Fourier transform of the dynamic density-density correlation function, which for lattice bosons is given by $\langle \delta n_j(t) \delta n_\ell(0) \rangle$ with $\delta n_j = n_j - \langle n_j \rangle$. It yields the linear response of the fluid to a density perturbation transferring a momentum $\hbar k$ and energy $\hbar \omega$ to the system. Its Lehmann representation reads

$$S(k, \omega) = \sum_{\alpha \neq 0} |\langle \alpha | n_k | 0 \rangle|^2 \delta(\omega - \omega_\alpha), \quad (3)$$

where α labels the eigenstates of the Hamiltonian (0 being the ground-state), $\omega_\alpha = E_\alpha - E_0$ are the excitation energies and

$$n_k = \sum_{j=1}^L e^{ikr_j} n_j \quad (4)$$

is the density operator at momentum k , with $r_j = a(j - L/2)$. On finite lattice systems with periodic boundary conditions we use $k = 2\pi m/L$ with integer m values. We will also consider the momentum integrated spectral function $S(\omega) = \sum_k S(k, \omega)$.

The dynamic structure factor can be experimentally probed by Bragg spectroscopy, involving a two-photon transition. Using the fluctuation-dissipation theorem, it can be extracted from the measured energy gain of the system per unit time dE/dt , according to [62, 29]

$$\frac{dE}{dt} \propto \omega S(k, \omega) \quad (5)$$

where ω is the frequency difference between the two photons involved in the transition and k is the wave-vector difference. Alternatively, the dynamic structure factor can be extracted from the rate of momentum transfer dP/dt [63]

$$\frac{dP}{dt} \propto k S(k, \omega). \quad (6)$$

Both definitions have been exploited to extract $S(k, \omega)$ in recent cold-atom experiments [64, 38, 65, 36, 39, 40]. It is worth mentioning that the f -sum rule allows to compare theory with experiment without adjustable parameters [27].

Three different theoretical approaches to compute $S(k, \omega)$ are used throughout this work and we describe them below.

2.3. Methods

2.3.1. Exact diagonalization We computed $S(k, \omega)$ using the Lanczos algorithm to represent the low-lying excited states. The method is exact but limited to small sizes. In the calculation, the maximum number of onsite bosons is fixed to 6, and 200 iterations are performed to compute the spectral weights. The delta functions in energy of the discretized excited states are convolved with lorentzians of width $0.2J$ for $S(k, \omega)$ and $0.3J$ for $S(\omega)$. Averaging is performed over 34 samples with a uniform ϕ distribution for the QP potential while 100 samples are used for the RB potential.

2.3.2. *Bogolyubov theory* For weakly interacting bosons having a finite condensate fraction in the ground state, it is well established that the ground-state properties as well as the low-energy excitation spectrum are well described within Bogolyubov theory. The traditional formulation of Bogolyubov theory requires the existence of a true condensate, and it amounts to neglecting terms which are not quadratic in the operators involving particles out of the condensate. Yet Ref. [66] has shown that an analogous approach to Bogolyubov theory can be applied to one-dimensional systems featuring only quasi-condensation. Such an approach is based on a polar decomposition of the Bose operators in terms of density and phase, $b_j = e^{i\phi_j} \sqrt{n_j}$, and on the fundamental assumption of weak quantum fluctuations of the density $\delta n_j = n_j - \rho_j$ around the mean ρ_j , as well as weak quantum fluctuations of the phase difference between neighboring sites $\theta_j - \theta_{j+1}$. The Hamiltonian can then be expanded in powers of the density and phase-difference fluctuations around a reference state, corresponding to non-fluctuating (and vanishing) phase differences and a classical density profile ρ_j which satisfies a lattice Gross-Pitaevskii (GP) equation

$$-J(\sqrt{\rho_{j+1}} + \sqrt{\rho_{j-1}}) + [U\rho_j - (\mu - w_j)]\sqrt{\rho_j} = 0. \quad (7)$$

Here μ is the chemical potential controlling the number of bosons in the system (see below) and ρ_j can be identified with the density profile of the quasi-condensate. Diagonalizing the quadratic Hamiltonian in the fluctuations amounts to a Bogolyubov transformation of the density and phase operators to operators a_s, a_s^\dagger

$$\begin{aligned} \delta n_j &= \sum_s (\delta n_{s,j} a_s + \delta n_{s,j}^* a_s^\dagger) + (\partial_N \rho_j) \mathcal{P} \\ \theta_j &= \sum_s (\theta_{s,j} a_s + \theta_{s,j}^* a_s^\dagger) - \mathcal{Q} \end{aligned} \quad (8)$$

where \mathcal{P} and \mathcal{Q} are canonically conjugated operators associated with the zero-energy mode, and

$$\delta n_{s,j} = \sqrt{\rho_j} (u_{s,j} + v_{s,j}) \quad \theta_{s,j} = \frac{u_{s,j} - v_{s,j}}{2i\sqrt{\rho_j}}. \quad (9)$$

The $u_{s,j}, v_{s,j}$ amplitudes satisfy the Bogolyubov-de Gennes (BdG) equations

$$\mathcal{L} \begin{pmatrix} |u_s\rangle \\ |v_s\rangle \end{pmatrix} = \begin{pmatrix} \mathcal{H}_2 & \mathcal{H}_U \\ -\mathcal{H}_U & -\mathcal{H}_2 \end{pmatrix} \begin{pmatrix} |u_s\rangle \\ |v_s\rangle \end{pmatrix} = \epsilon_s \begin{pmatrix} |u_s\rangle \\ |v_s\rangle \end{pmatrix} \quad (10)$$

where

$$\begin{aligned} \mathcal{H}_2 &= -J \sum_j (|j\rangle\langle j+1| + \text{h.c.}) + \sum_j (2U\rho_j + w_j - \mu) |j\rangle\langle j| \\ \mathcal{H}_U &= \sum_j U\rho_j |j\rangle\langle j| \end{aligned} \quad (11)$$

and $|u_s\rangle = \sum_j u_{s,j} |j\rangle$, $|v_s\rangle = \sum_j v_{s,j} |j\rangle$. The properties of the non-Hermitian eigenvalue problem of Eq. (10) are well known [67]; in particular the solutions of the BdG equations with non-zero energy ϵ_s satisfy the normalization condition

$$\langle u_s | u'_s \rangle - \langle v_s | v'_s \rangle = \delta_{ss'}. \quad (12)$$

In the absence of disorder the u and v modes are plane waves, and the corresponding energies, labeled by momentum ($s \rightarrow k$), have the well-known form

$$\omega_k = \sqrt{e_k(e_k + 2nU)}, \quad \text{with} \quad e_k = 4J \sin^2(k/2). \quad (13)$$

Given that quantum fluctuations in the density are linear in the a_s, a_s^\dagger operators, within the quadratic approximation for quantum fluctuations the quantum corrections to the density profile vanish (which is consistent with the image of ρ_j as the mean local density). Therefore the total particle number is given by $N = \sum_j \rho_j$, and the chemical potential μ in Eq. (7) is fixed so as to impose the desired lattice filling at the level of the GP equation.

The Bogolyubov theory for quasi-condensates of Ref. [66] has been applied to 1D Bose gases in a disordered potential in a number of recent papers [68, 69, 70, 71]. In particular Refs. [68, 69, 72] provide an explicit expression for the one-body density matrix, $g^{(1)}(j, l) = \langle b_j^\dagger b_l \rangle$ in terms of the solution of the GP and BdG equations, reading

$$g^{(1)}(j, l) = \langle b_j^\dagger b_l \rangle = \sqrt{\rho_j \rho_l} \exp \left[-\frac{1}{2} \sum_s \left(\frac{v_{s,j}^\perp}{\sqrt{\rho_j}} - \frac{v_{s,l}^\perp}{\sqrt{\rho_l}} \right)^2 \right] \quad (14)$$

where $u_{s,j}^\perp, v_{s,j}^\perp$ are the coefficients of the vectors $|u_s\rangle, |v_s\rangle$ orthogonalized with respect to the quasi-condensate

$$|u_s^\perp\rangle = |u_s\rangle - \langle \psi_0 | u_s \rangle | \psi_0 \rangle \quad (15)$$

(and similarly for $|v_s^\perp\rangle$). Here $|\psi_0\rangle = \sum_j \psi_{0,j} |j\rangle$ is the normalized quasi-condensate mode, with $\sqrt{\rho_j} = \sqrt{N} \psi_{0,j}$.

The calculation of the dynamic structure factor of a weakly interacting Bose gas has been addressed within Bogolyubov theory in various references [73, 74]. In the case of quasi-condensates its expression turns out to be analogous to that of conventional Bogolyubov theory [74], namely

$$S(k, \omega) = \sum_s |\delta \tilde{\rho}_s(k)|^2 \delta(\omega - \epsilon_s) \quad (16)$$

where the form factors $\delta \tilde{\rho}_s(k)$ read

$$\delta \tilde{\rho}_s(k) = \sum_j e^{-ikr_j} \sqrt{\rho_j} (u_{s,j} + v_{s,j}). \quad (17)$$

Notice that here we restrict our attention to the case $\omega > 0$, so that the zero-mode contributions disappear from $S(k, \omega)$. In the absence of an external potential, the dynamic structure factor is a δ -peak resonance at the Bogolyubov mode ϵ_k [21]:

$$S(k, \omega) = \frac{e_k}{\omega_k} N \delta(\omega - \omega_k). \quad (18)$$

The Bogolyubov theory for quasi-condensates is quantitatively consistent as long as the quantum fluctuations of the density and relative phase remain weak. In particular,

the phase-density formulation requires the condition $\rho_j \gg 1$ to be fulfilled in order for the phase operator to be well defined as a (quasi-)Hermitian operator [66]. Moreover, a large quasi-condensate density on each site is also necessary for the relative particle fluctuations to be small, since $\langle(\delta n_j)^2\rangle/\rho_j^2 \geq 1/\rho_j$ [66]. As we will see, this condition will strongly limit the range of validity of our results.

From the practical point of view, we numerically solve the Gross-Pitaevskii equation via split-operator imaginary-time propagation, and the Bogolyubov-de Gennes equations by diagonalization of the non-Hermitian \mathcal{L} matrix using the LAPACK libraries, as described in previous references [75]. We present results for lattices with $L = 256$ and $L = 512$ sites. Unless otherwise specified, the results for QP potentials are averaged over ~ 50 values of the spatial phase ϕ of the potential.

2.3.3. Hardcore-boson limit While Bogolyubov theory applies to weakly interacting bosons at large filling, we can also consider the opposite limit of infinitely repulsive bosons, $U \rightarrow \infty$, and low filling $n < 1$. This limit corresponds to the 1D Tonks-Girardeau gas of hardcore bosons (HCB), in which the forbidden double occupancy of the sites can be incorporated in a redefinition of the bosonic operators, $b_i \rightarrow \tilde{b}_i$ satisfying bosonic commutation relations offsite and anticommutation relations onsite, $[\tilde{b}_j, \tilde{b}_l^{(\dagger)}] = 0$ for $j \neq l$ and $\{\tilde{b}_j, \tilde{b}_j^\dagger\} = 1$, $\{\tilde{b}_j, \tilde{b}_j\} = \{\tilde{b}_j^\dagger, \tilde{b}_j^\dagger\} = 0$. The hardcore boson operators $\tilde{b}_j^{(\dagger)}$ can be transformed to fermionic ones $c_j^{(\dagger)}$ via a Jordan-Wigner transformation [76], mapping exactly the hardcore boson Hamiltonian to free fermions with chemical potential μ

$$\mathcal{H} = -J \sum_j \left(c_j^\dagger c_{j+1} + \text{h.c.} \right) + \sum_j (w_j - \mu) c_j^\dagger c_j \quad (19)$$

which lends itself to efficient exact diagonalization. In the following we will focus on systems with open boundaries or in a trap, and therefore we omit in the Hamiltonian the boundary terms arising from the non-local nature of the Jordan-Wigner transformation.

Most notably, the hardcore boson density coincides with the fermionic one, $\tilde{b}_j^\dagger \tilde{b}_j = c_j^\dagger c_j$, so that the dynamic structure factor of the hardcore bosons corresponds to that of the free fermions, taking the simple expression

$$S(k, \omega) = \sum_{\alpha\beta} |\rho_{\alpha\beta}(k)|^2 f(e_\beta, T) [1 - f(e_\alpha, T)] \delta(\omega - \omega_{\alpha\beta}) \quad (20)$$

where $\omega_{\alpha\beta} = e_\alpha - e_\beta$, e_α are the eigenenergies of the single particle problem in the QP potential, $f(e, T) = \{\exp[(e - \mu)/(k_B T)] + 1\}^{-1}$ is the Fermi-Dirac occupation factor at a finite temperature T , and

$$\rho_{\alpha\beta}(k) = \sum_j e^{ikr_j} \psi_{\alpha,j}^* \psi_{\beta,j} . \quad (21)$$

Hence we observe that, for hardcore bosons, the k -dependence of the dynamic structure factor describes the power spectrum in momentum space of the overlap function $\psi_{\alpha,j}^* \psi_{\beta,j}$ between occupied and unoccupied single-particle states, connected by the energy transfer $\hbar\omega$.

3. Dynamic structure factor of the clean system: superfluid and Mott phases

The phase diagram of the clean Bose-Hubbard model displays two phases [19]: the superfluid phase (SF) which occurs generically at incommensurate densities, and the Mott-insulator (MI) phase which occurs only at commensurate fillings and beyond a critical interaction strength U_c (for a one-dimensional system with filling $n = 1$, $U_c \simeq 3.3J$). In the incommensurate case at densities $n < 1$, there are two main types of low-energy excitations contributing to the dynamic structure factor in the Bose-Hubbard model. The first type is represented by gapless acoustic modes related to the superfluid regime and which have, in the long wavelength limit, the dispersion relation $\omega(k) \simeq ck$, with c the sound velocity. The second type is represented by doublon excitations, namely repulsively bound states of two particles occupying the same site, occurring when the repulsion energy exceeds the bandwidth; these bound states appear at the two-body level, and survive in the many-body case [77]. Its energy creation cost is about $4J + U$ in the strong coupling limit. In the Mott regime, the elementary excitations form a particle-hole continuum. This gapped excitations of the Mott phase have a typical energy cost of the order of U and the shape of the particle-hole continuum is known in the deep Mott limit (see e.g. Ref. [27]). This excitation is essential in understanding the dynamical properties of the system at large U , and it is the main excitation in the Mott phase where sound modes are absent.

These elementary excitations are visible in the dynamic structure factor of the clean Bose-Hubbard model. We give in Fig. 1(a) the evolution of the dynamic structure factor $S(k, \omega)$ for increasing interaction U/J and for two typical densities: incommensurate ($n = 0.5$) and commensurate ($n = 1$).

We start with the incommensurate case. At small U/J , we display the Bogolyubov result of Eq. (18). The overall behavior has a form of an arc on $[0, 2\pi]$ due to the periodicity in momentum space. For $U = 2J$, we see that the Bogolyubov result and the exact diagonalization result differ qualitatively. While it is expected that Bogolyubov theory fails to account for such a relatively strong interaction, we observe that the essential difference emerges around $k \sim \pi$ where local physics is dominant. The spectrum is there split into two lines which we interpret as an hybridization between the acoustic modes and the gapped doublon state. Then, the peak emerging on top of the acoustic branch is attributed to the doublon state. This doublon mode is roughly centered around the energy $4J + U$, as we see for increasing U/J , and as expected for repulsively bound pairs [77]. When its energy increases, its spectral weight decreases, as one can see from $S(\omega)$ plotted in Fig. 1(b). In addition, increasing the interaction strength transfers spectral weight to the low-energy states at the $k = 2k_F$ wave vector, $k = 2\pi n$ (*i.e.* $k = \pi$ in the figure) corresponding to back-scattering (see eg [78]). This is the very analogue of what is found in the Lieb-Liniger model [22] in the absence of the lattice. In the hardcore boson limit, the spectrum corresponds to the XX spin chain model which displays the famous Pearson-De Cloiseaux continuum (see e.g. [79, 27]).

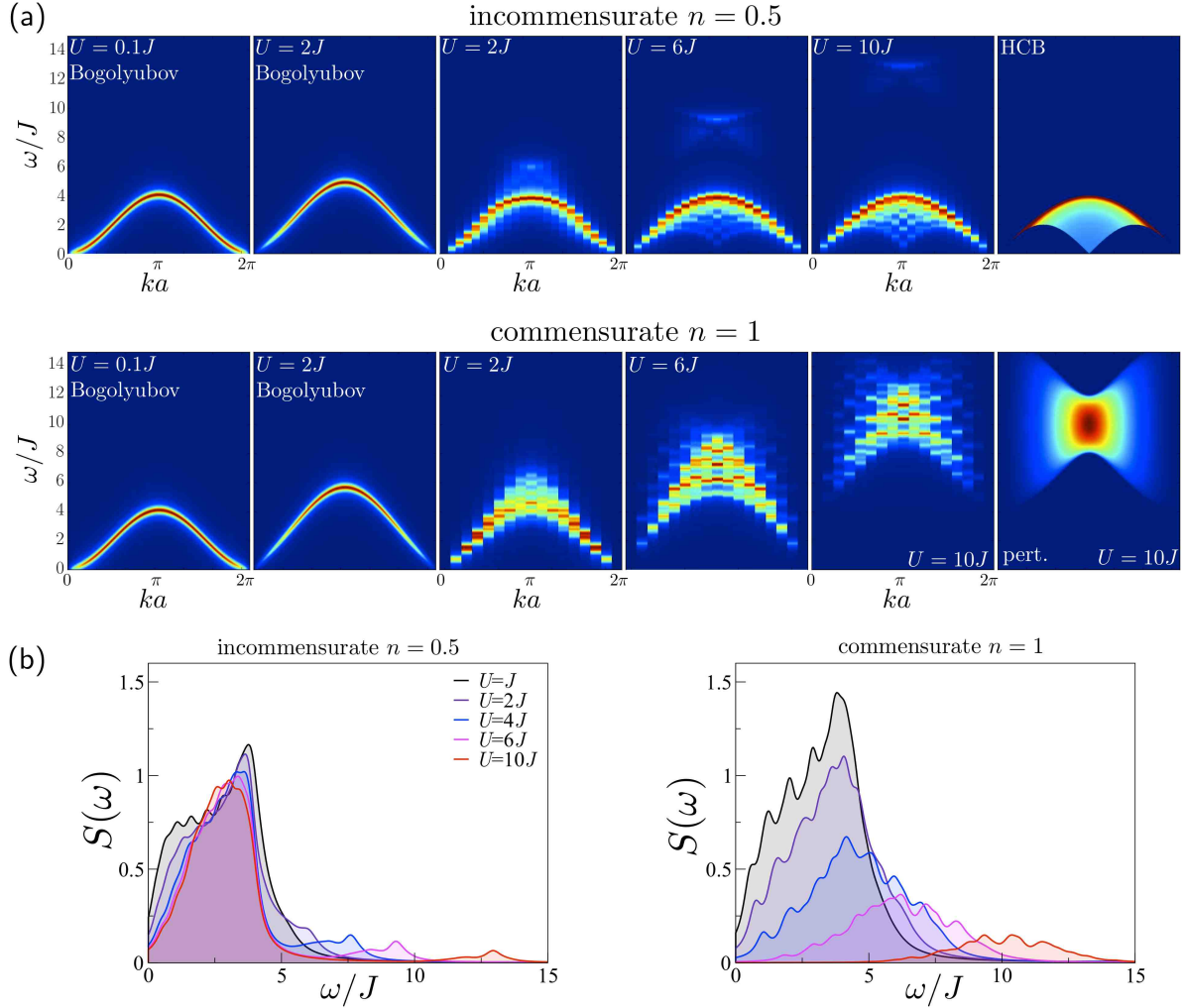


Figure 1. (a) Dynamic structure factor $S(k, \omega)$ for the clean system. Upper panel: for an incommensurate filling $n = 0.5$ ($L = 22$) from weak to strong interactions. Bogolyubov and hardcore-boson (HCB) results are compared to exact diagonalization. Lower panel: for a commensurate filling $n = 1$ ($L = 16$) where the Mott phase emerges at large U/J . The perturbative (pert.) result is also shown. Color scales from different figures are different. (b) Integrated dynamic structure factor $S(\omega)$, allowing to compare the spectral weights for different U/J for the two situations.

In this limit, the doublon excitation is no longer part of the spectrum. Thus, exact diagonalization nicely interpolates between the two regimes, and it exhibits the evolution of the doublon excitation in the spectrum when approaching the HCB limit.

Looking at the commensurate $n = 1$ case in Fig. 1, one can see the transition from the SF to the MI phase when interactions are increased, although the opening of the gap in the dispersion relation is appreciable only at U sizably larger than U_c because of finite-size effects (the gap opens exponentially slowly). One switches from the SF behavior at $U = J$, similar to the incommensurate case and in qualitative agreement with Bogolyubov theory, to a fully gapped excitation spectrum in the MI regime which corresponds to the particle-hole dispersion centered around $\omega \sim U$. For

$U = 2J$, there is a single peak in the acoustic mode, with a short lifetime at $k = \pi$ compatible with previous results for the same filling [33, 34, 35]. Interestingly, in the intermediate interaction regime $U \sim 6J$, the system is gapped but the particle-hole dispersion has a significant weight at the lowest frequencies, reminiscent of the acoustic mode spectrum [28]. According to perturbation theory [27], for large enough U/J the spectrum is predicted to display a butterfly-like shape with a maximum weight around $k = \pi$. For $U = 10J$, where the gap is sizeable, $S(k, \omega)$ has a similar support as the perturbative prediction of Ref. [27], but the weight distribution is not yet symmetric around $\omega = U$. We observe that ED can quantitatively covers the evolution of $S(k, \omega)$ from the weakly to the strongly interacting regime, and that Bragg spectroscopy can capture the opening of the gap. Yet, in realistic conditions with a trap, one would have to consider the effect of the inhomogeneity of the system [27].

4. Dynamic structure factor for the quasi-periodic system

The impact of disorder on elementary excitations of interacting bosons can be expected to be qualitatively similar to that on single-particle states, leading in particular to localization of the spatial support of the excitation modes. The connection between single-particle and many-body physics is evident within the Bogolyubov and HCB approaches, since the spatial structure of the excitation modes comes from the solution of the single-particle Schrödinger's equation (for HCB) or the solution of BdG equations in the presence of a (quasi-)disordered potential. Yet the same connection is far less obvious in the full Bose-Hubbard model. In what follows we will first describe our results in the Bogolyubov and HCB regimes, and then show how exact diagonalization allows to interpolate between the above regimes. In the case of exact diagonalization we also compare the case of QP and RB potentials, and we show that, due to the different nature of the localization mechanism at play, these two potentials lead to very distinct features in the dynamic structure factor.

4.1. Results from Bogolyubov theory

We present here the results for the dynamic structure factor of one-dimensional weakly interacting bosons in a quasi-periodic lattice. We begin our discussion with the non-interacting limit, which serves as a useful reference for the results in the interacting case.

4.1.1. $U=0$ In the case of an ideal gas, the dynamic structure factor takes the simple form

$$S(k, \omega) = \sum_{\alpha} |\rho_{\alpha 0}(k)|^2 \delta(\omega - \omega_{\alpha}) \quad (22)$$

where \sum_{α} runs over the single-particle eigenstates, $\omega_{\alpha} = e_{\alpha} - e_0$ is the excitation energy of the α state, and e_{α} is the single-particle eigenenergy corresponding to the lattice

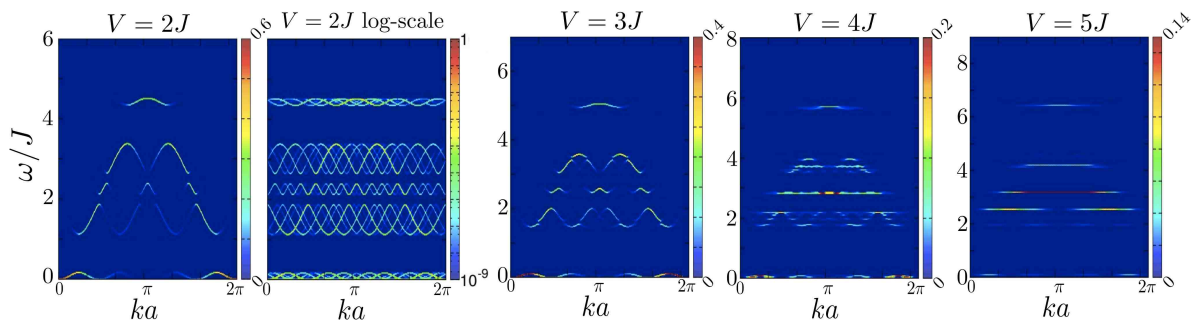


Figure 2. Dynamic structure factor $S(k, \omega)$ for free bosons in a quasi-periodic potential for increasing strength V/J of the disorder potential. The case $V = 2J$ is shown in log-scale to highlight the underlying excitations bands.

eigenfunction $\psi_{\alpha,j}$; $\rho_{\alpha 0}(k)$ is the Fourier transform of the overlap function between the ground-state and the α -th excited state, defined in Eq. (21).

If the ground-state is close to a $k = 0$ plane wave, the $\rho_{\alpha 0}(k)$ form factor is essentially proportional to the Fourier transform of the excited state ψ_{α} . As a consequence $S(k, \omega)$ gives the power spectrum in momentum space for the excited state at energy $\epsilon_{\alpha} = \omega$. Therefore, even in the absence of translational invariance (broken by the QP potential), the presence of a sharp ridge in $S(k, \omega)$ gives an effective energy-momentum dispersion relation for the excited states of the system.

Fig. 2 shows the single-particle dynamic structure factor for an increasing strength of the QP potential. We observe that the $e_{\alpha} = e_k$ dispersion relation of free particles in the lattice, characterized by a single cosine band, breaks up into sub-bands for a finite V . We shall first focus on the delocalized phase $V < V_c$. The appearance of the sub-bands can be related with the fact that the QP potential introduces a quasi-periodic structure in the lattice, whose spatial period corresponds to the period of the beating between the underlying lattice and the incommensurate potential, $l_{\text{QP}} = (1 - r)^{-1}$. Correspondingly features in momentum space appear at the edges of a (pseudo-)Brillouin zone with width $k_{\text{QP}} = 2\pi(1 - r)$, namely at $k_{\text{QP}}/2, \pi \pm k_{\text{QP}}/2$, etc.; these are indeed the (approximate) momentum locations at which the gaps between the sub-bands appear in $S(k, \omega)$. Within each subband the excitations are delocalized with sharp momentum content, and they exhibit a cosine-like dispersion with the periodicity of the pseudo-Brillouin zone. Yet, due to the incommensurability, the pseudo-Brillouin zone cannot fill the Brillouin zone of the underlying lattice an integer number of times, and hence the sub-bands dispersion curves essentially fade away in $S(k, \omega)$ after a few periods (in fact a closer inspection shows that they persist over the whole Brillouin zone, and they even wind around it giving rise to a very complex pattern, which nonetheless is only seen in logarithmic scale – see Fig. 2 for $V = 2J$). This fading dispersion relation can be understood within a perturbative picture for the QP potential: a particle with momentum k and energy e_k (in the absence of the QP potential) is scattered by the QP potential and it can acquire a momentum $p k_{\text{QP}}$ at p -th order in perturbation theory, but due to the incommensurability there is no finite order in perturbation theory

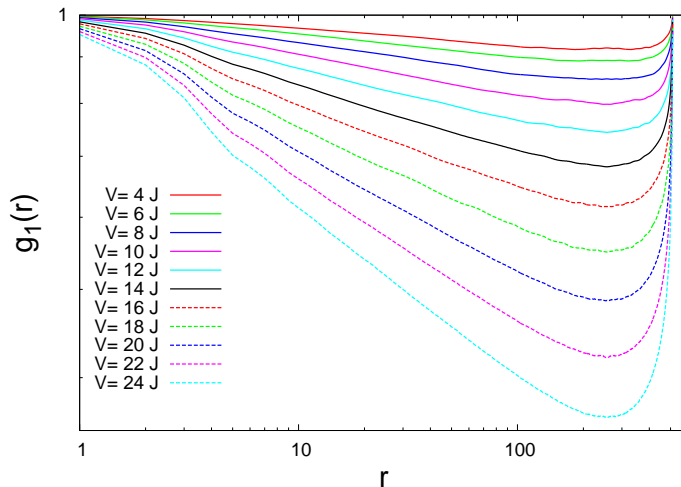


Figure 3. One-body density matrix for the 1D weakly interacting lattice Bose gas in a QP potential of increasing strength. The parameters are $r = 395/512$, $U = 0.1J$, $n = 10$, and $L = 512$.

which can connect the initial state to a resonant unperturbed state, and therefore the particle remains “localized” around its initial momentum k with fading components at $k \pm k_{\text{QP}}$, $k \pm 2k_{\text{QP}}$, etc. This picture of localization in momentum space is valid beyond perturbation theory, and it relies on the exact duality of the non-interacting model under Fourier transformation [16, 50].

For $V > V_c$, $S(k, \omega)$ undergoes a radical change: the dispersive nature of the excitations within the subbands disappears, and $S(k, \omega)$ acquires features which are very broad in momentum space, while retaining a sharp nature in the frequency domain. This corresponds to the appearance of strongly localized modes, possessing a large uncertainty in momentum space. The large broadening of the structure of $S(k, \omega)$ in momentum space is therefore the signature of localization, and it will reappear as a leitmotiv in the analysis of the results for the interacting system.

4.1.2. $U > 0$. In the following we present our results for the weakly interacting case. We will mostly present results for $U = 0.1J$ and a lattice filling $n = 10$ to satisfy the conditions of validity of Bogolyubov theory – although we have also investigated the interaction strengths $U = 0.01J$ and $0.5J$, displaying similar features to $U = 0.1J$. As already discussed in Refs. [80, 68, 69, 81] for the case of bosons in continuum space, Bogolyubov theory is capable of describing quasi-condensates, and specifically a power-law decaying one-body density matrix. This is also verified for a lattice system and in the presence of a QP potential, as shown in Fig. 3. In particular we observe that weak interactions make the quasi-condensate state robust to the QP potential, and they promote it to values of V well beyond the critical value $V_c = 4J$ for the non-interacting system. In the case of a 1D gas in continuum space and subject to a speckle or quasi-periodic potential, Refs. [68, 69, 81] have shown that Bogolyubov theory allows

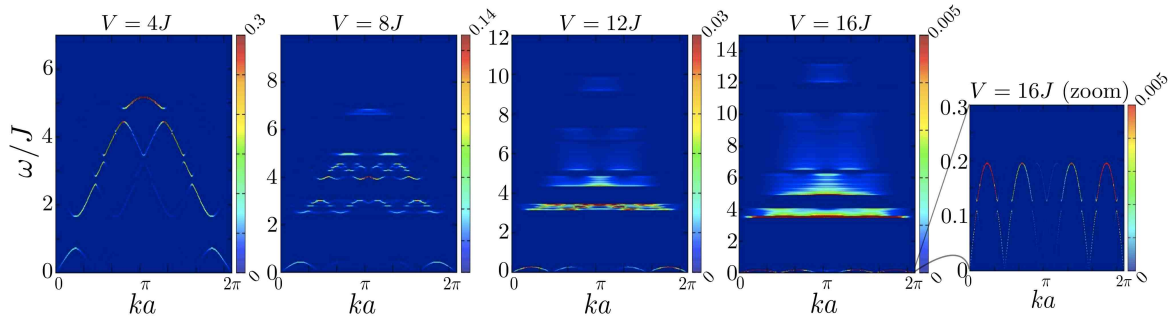


Figure 4. Dynamic structure factor $S(k, \omega)/N$ for the 1D weakly interacting lattice Bose gas in a QP potential of increasing strength. Same parameters as in Fig. 3.

to quantitatively describe the localization transition in one dimension in the presence of interactions; such a transition is detected by the appearance of an exponential decay in the one-body density matrix. This has allowed the authors of Refs. [68, 69, 81] to track the interaction-induced shift of the critical disorder strength. In the lattice system under investigation, on the other hand, we rather find that Bogolyubov theory fails to reproduce quantitatively this transition. Indeed, for all the interaction strengths we considered, we find that a quasi-condensate phase is observed over the whole range of applicability of the theory, namely for disorder strengths V which do not lead to excessive fragmentation of the density profile. Indeed, if the disorder strength is too large, there will appear sites in the lattice with $\rho_i \ll 1$, clearly violating the condition of weak density fluctuations. We do observe a change of the $g^{(1)}$ function from an algebraic to an exponential decay with increasing V , but this occurs at unrealistically large values of V , well beyond the value $\sim V_c + Un$ which naïvely represents the critical value for a QP potential screened by the interactions, and well beyond the range of validity of the theory.

Even if Bogolyubov theory does not allow us to describe the localized Bose glass phase for the ground state of the system under investigation, it still reveals a dramatic evolution in the properties of the excitations, and a very peculiar nature of the persistent quasi-condensate phase protected by the interactions. The evolution of the dynamic structure factor for an increasing strength of the QP potential is shown in Fig. 4. When comparing it to the non-interacting case of Fig. 2, one clearly observes substantial analogies. In particular under the effect of the QP potential, Bogolyubov modes are still organized in sub-bands, which exhibit sharp dispersion relations in the (k, ω) plane for sufficiently weak V , while they lose completely their definition in momentum space when the modes undergo localization for a larger value of V . We observe that the modes at *higher* energy localize at a *lower* value of V , as we will further elaborate upon in the following. In particular the lowest sub-band, containing the gapless excitation modes above the ground state, preserves its dispersive nature for all the values of the QP potential considered, even if the bandwidth gradually decreases with V - this is exhibited in Fig. 4 for $V = 16J$, where a low-energy zoom on $S(k, \omega)$ is presented for the two strongest values of V shown in Fig. 4. In particular the effective dispersion relation of

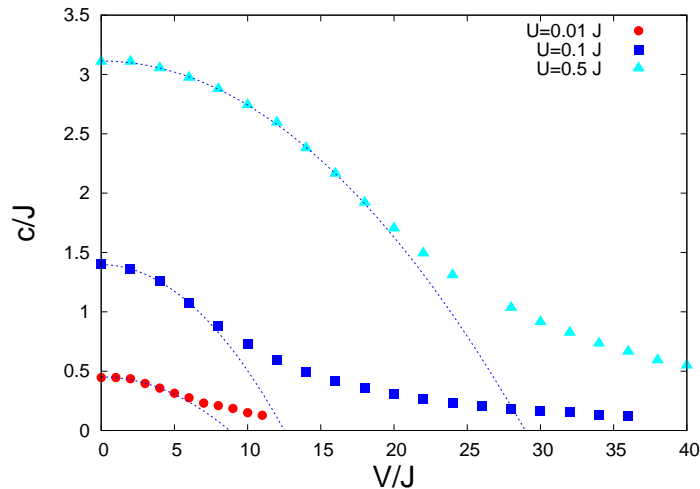


Figure 5. Sound velocity as a function of the QP potential strength and for various values of the inter-particle repulsion. Other parameters as in Fig. 4. The dashed curves are parabolic fits $c(V) = c(0) - \gamma V^2$ for the lowest V values.

the lowest band preserves a linear behavior for $k \rightarrow 0$, characteristic of a delocalized sound mode. From the slope at $k \rightarrow 0$, we extract an effective sound velocity c , which is shown in Fig. 5. We find that c decreases as $c(V) \approx c(0) - \gamma(U, n) V^2$ where γ is a constant; this is consistent with the perturbative results of Ref. [82, 83], showing that the quadratic dependence on V is a generic property of Bogolyubov modes in the presence of an external scattering potential.

The progressive localization of Bogolyubov modes from the higher to the lower energies upon increasing the QP potential can be quantitatively captured by inspecting the effective spatial support of the u and v lattice functions. Following the natural definition of norm for the u, v functions as in Eq. (12), and in analogy with the case of normalized wave functions, one can define a participation ratio (PR) for the u, v functions in the form

$$\text{PR}_{uv}(\omega) = \frac{1}{L} \frac{\left[\sum_j (u_{s,j}^2 - v_{s,j}^2) \right]^2}{\sum_j (u_{s,j}^2 - v_{s,j}^2)^2} = \frac{1}{L} \frac{1}{\sum_j (u_{s,j}^2 - v_{s,j}^2)^2}. \quad (23)$$

This quantity captures the fraction of the system size over which the u, v functions have a non-negligible value. Fig. 6(a) shows the evolution of PR_{uv} as a function of both QP potential strength and excitation energy: it is clear that for every finite value of V the high-energy Bogolyubov modes are more localized than the low-energy ones, and in particular for $V \sim 6J$ the highest band of Bogolyubov modes undergoes localization, and the lower bands follow in the localization cascade at higher V , while the lowest band remains delocalized over the entire range of V values covered by the figure.

Coming back to the dynamic structure factor, its expression, Eq. (16), probes the spatial structure of the overlap function $\sqrt{\rho_j}(u_{s,j} + v_{s,j})$ - giving the local overlap between the quasi-condensate mode and the excitation mode - and not simply the spatial

structure of the u, v functions. Nonetheless, if the condensate mode is delocalized, then the overlap function has the same localization properties as the u, v functions. This can be directly inspected by plotting the participation ratio for the overlap function:

$$\text{PR}_{uv0}(\omega) = \frac{1}{L} \frac{\left[\sum_j \sqrt{\rho_j} (u_{s,j} + v_{s,j}) \right]^2}{\sum_j \rho_j (u_{s,j} + v_{s,j})^2}. \quad (24)$$

As shown in Fig. 6(a), the behavior of this quantity (as a function of QP potential strength and mode energy) is qualitatively very similar to the participation ratio of the u, v functions of Eq. (23). As a consequence, the dynamic structure factor can capture the localization properties of the u, v functions given that in its expression, Eq. (16), the Bogolyubov modes at energy ϵ_s are weighted by the power spectrum $|\delta\tilde{\rho}_s(k)|^2$ of the overlap function. In particular the power spectrum has opposite localization properties with respect to the overlap function, namely it is delocalized in k space when the overlap function is localized and vice versa. Therefore, it appears natural that the localization properties of the overlap function can be extracted from the dynamic structure factor by examining its *inverse* participation ratio (IPR) of in k space

$$\text{IPR}_S(\omega) = \frac{\sum_k S^2(k, \omega)}{S^2(\omega)}. \quad (25)$$

In particular one can easily show that $S(\omega) = L \sum_j \rho_j (u_{s,j} + v_{s,j})^2$, so that IPR_S and PR_{uv0} share the same denominator. Fig. 6(b) shows IPR_S as a function of V and ω ; a comparison with the (V, ω) dependence of PR_{uv0} shows striking similarities, demonstrating that the dynamic structure factor allows to measure directly the localization properties of the excitation modes in the Bogolyubov regime.

4.2. Results for hardcore bosons

4.2.1. Weak QP potential.

For a weak QP potential the (pseudo-)dispersion relation of single particles is altered as discussed in Section 4.1.1, with the opening of gaps at $k_{\text{QP}}/2$, $\pi \pm k_{\text{QP}}/2$, etc... In Fig. 7 we show the dynamic structure factor for hardcore bosons of variable density in a weak QP potential $V = 0.25J$. In one-dimensional free fermions, some of the dominant features in the structure factor are related to the transitions between the states at the bottom of the dispersion relation and states anywhere else in the energy spectrum - this is due to the singular contribution of the low-energy states, associated with the van-Hove singularity in their density of states. As a consequence we observe all single-particle gaps in the dynamic structure factor as long as Pauli principle allows the corresponding transitions, namely as long as the Fermi wave vector, $k_F = \pi n$, is lower than the wave vector of the arrival state - otherwise the transition is forbidden by Pauli blocking. Indeed we see that the gap at $k \approx k_{\text{QP}}/2$ disappears when $k_F > k_{\text{QP}}/2$ (corresponding here to $n \gtrsim 0.23$), and the low- k and low- ω structure factor is dominated by the linear mode with dispersion $2J \sin(k_F) k$. In what follows we will focus on this situation, and investigate the case of (local) filling $n \approx 0.3$.

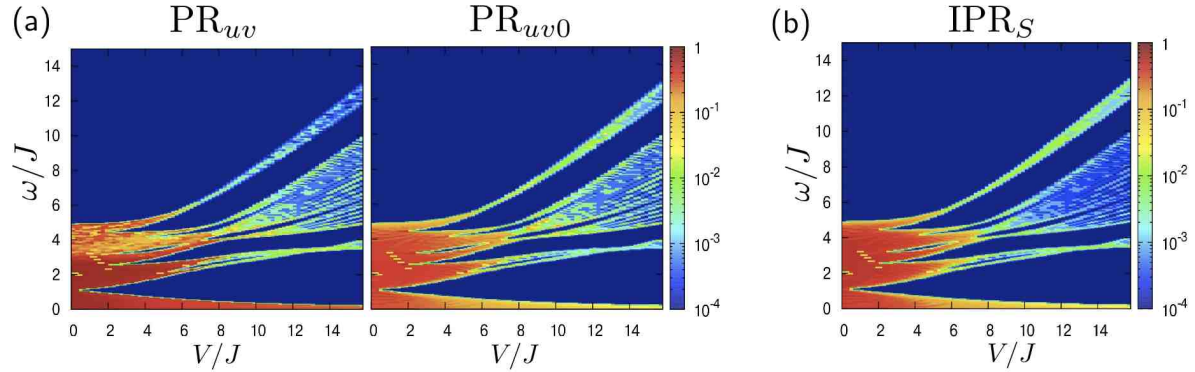


Figure 6. (a) Participation ratios PR_{uv} and PR_{uv0} (see text for the definition) of variable V and ω . Here $U = 0.1$, $r = 198/256$ and $L = 256$; the data are referred to one single realization of the phase of the QP potential. The energy axis is discretized into intervals of width $\delta\omega = 0.02J$, and the participation ratios (PRs) shown in the figure are an average of the values of the PR for the various modes falling within the energy interval. The dark-blue regions - associated with a vanishing PR - correspond to the gaps between Bogolyubov bands. (b) Inverse participation ratio of the dynamic structure factor; same parameters as in the previous panel.

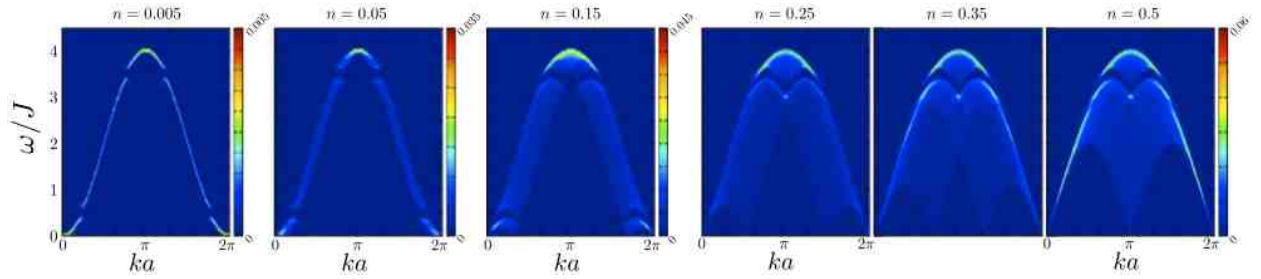


Figure 7. Dynamic structure factor for hardcore bosons in a QP potential with strength $V = 0.25J$. Here we consider an open chain with $L = 200$ and variable density, and a single realization of the QP potential.

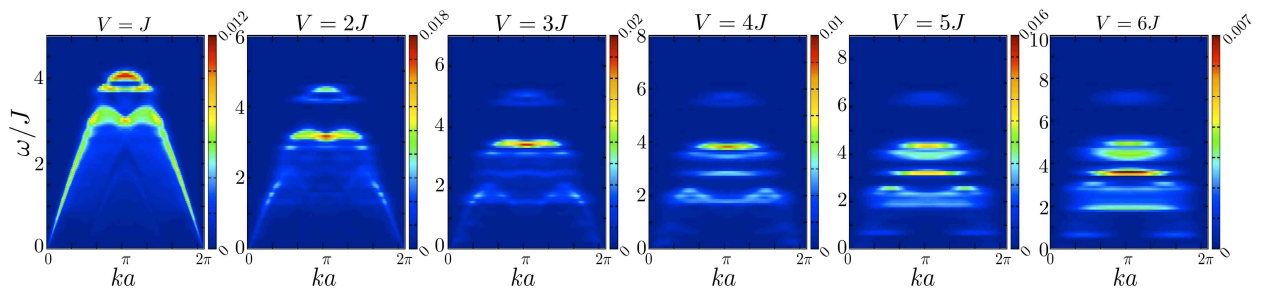


Figure 8. $T = 0$ dynamic structure factor of 1D hardcore bosons in a QP potential with variable strength, and in the presence of a confining parabolic potential.

4.2.2. Strong QP potential and localization transition. In the presence of a QP potential with strength $V > 4J$ all single-particle states localize, and therefore we expect a radical change in the k dependence of the form factors $\rho_{\alpha\beta}(k)$ in Eq. 20, as the overlap functions $\psi_{\alpha j}^* \psi_{\beta j}$ evolve from extended to localized. This is indeed observed

in Fig. 8 where we consider the evolution of the dynamic structure factor across the localization transition at $T = 0$ for a system of $N = 60$ hardcore bosons in a QP potential, and further confined by a weak harmonic potential $V_t r_j^2$ (to make contact with an experimentally realistic situation) with $V_t = 10^{-3}J$. We observe that the dispersive nature of the excitation modes is quickly lost as V approaches the critical value, and that the structure factor fragments into horizontal ridges, namely excitation modes which are well defined in energy but poorly defined in momentum space. Such features correspond predominantly to localized particle-hole excitations, in which the two states ψ_α and ψ_β connected by the transition are both localized in the same region of the system, giving a sizable overlap function.

4.3. Exact diagonalization results: competition between Mott insulator and Bose glass, and comparison between QP and RB potentials

4.3.1. Exact diagonalization results for QP potentials We now turn to the results of exact diagonalization in the QP case. The dynamic structure factor is given in Fig. 9 for four typical situations with increasing QP potential: incommensurate with weak and strong interactions (Fig. 9(a)), and commensurate for the same interaction regimes (Fig. 9(b)). In the incommensurate case, the effect of the bichromatic potential is rather weak at $U = 2J$ and $V = 2J$. The ω width increases and the doublon mode is hardly visible but one does not see the opening of gaps expected from Bogolyubov theory, possibly because of finite size effects. Increasing further the potential leads to localization of the excitations and a spectrum qualitatively similar to the one predicted using the Bogolyubov approach in Sec. 4.1.2. Notice that although the spectrum apparently looks gapped due to a large spectral weight for excitations at $\omega \sim 3J$, it is in fact gapless but with small weights for low-energy excited states. The effect of the QP potential is more evident when starting from $U = 10J$ (close to the HCB limit) and increasing V . Subbands in the spectrum do appear (see the panel with $U = 10J$, $V = 2J$ in Fig. 9) while the doublon mode loses some of its dispersive features, consistently with the fact that it can be localized already at weak QP potential strength – it has a reduced effective hopping $\sim J^2/U$ – and its energy is lowered by the disorder. For a strong QP potential ($V = U$), the spectrum exhibits many subgaps and it strongly broadens in k , in a very similar manner to what seen in the HCB results of Sec.4.2. The doublon mode is no longer resolved and the spectrum has large weights over a broad range of frequencies, while the integrated weight $S(\omega)$ shows a strong suppression.

Turning to the commensurate case in the superfluid regime ($U = 2J$), here again a sufficiently large bichromatic potential is required to change the spectrum. Above the localization transition, the spectrum displays many subgaps typical of the band-folding localization mechanism (as seen in the panel for $U = 2J$, $V = 10J$ in Fig. 9(b)) before reaching similar strongly localized spectrum as in the incommensurate density at very large V (see the $V = 20J$ panel). Starting from the MI phase at $U = 10J$, and introducing a weak QP potential ($V = 2J$ in Fig. 9(b)), we observe that the spectral gap

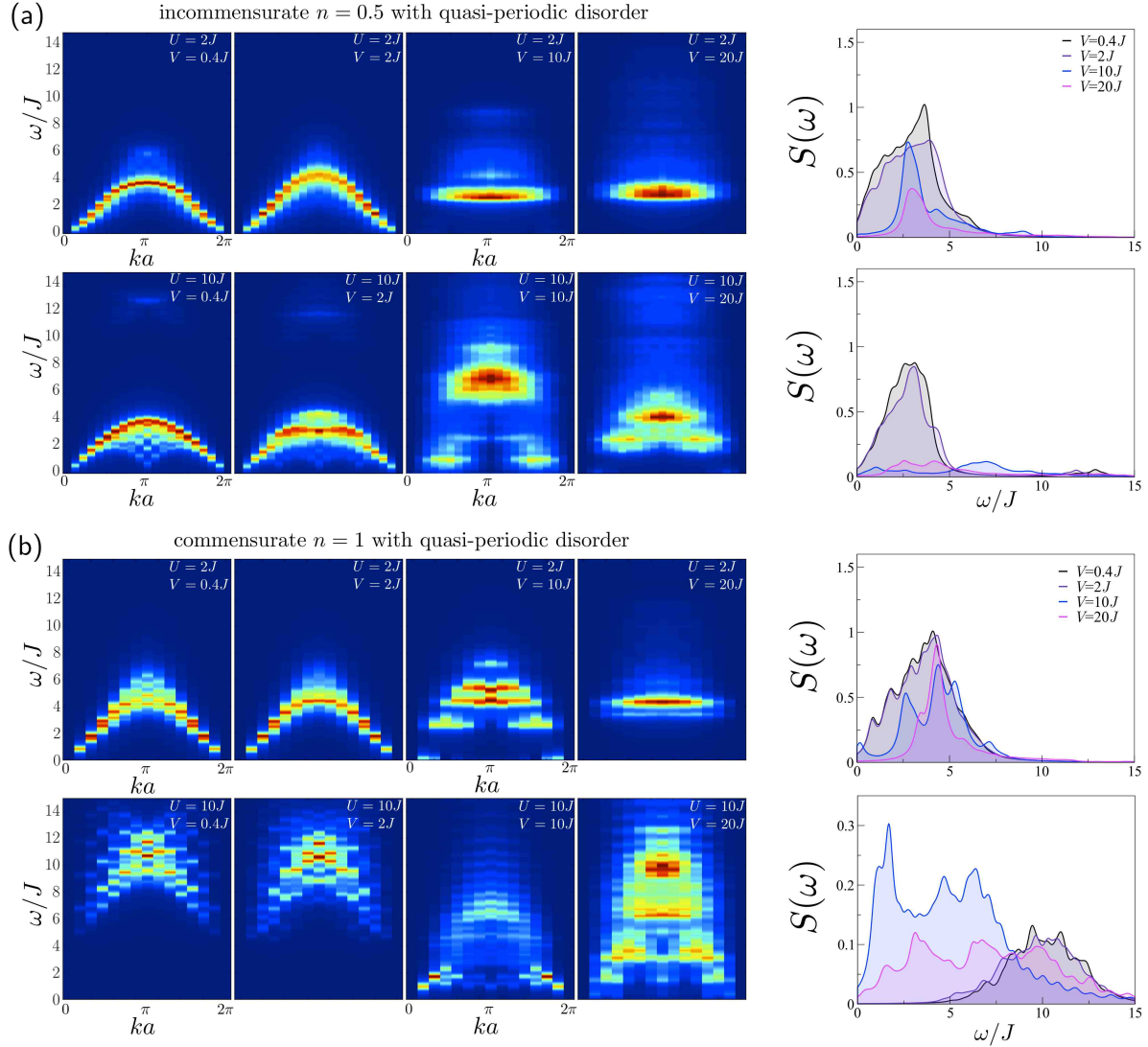


Figure 9. Dynamic density structure factor for the bichromatic system. (a) for a typical incommensurate density $n = 0.5$ ($L = 20$). (b) for the commensurate density $n = 1$ ($L = 14$) where the Mott phase emerges at large U/J .

is initially lowered, and mini-gaps appears in the particle-hole dispersion. For a stronger QP potential ($V = U = 10J$ in Fig. 9(b)), the gap closes and the system enters the strongly-correlated Bose glass phase. The spectrum exhibits both low-energy excitations with weights around $k = 0$ - corresponding to phonon-like modes of locally superfluid regions - and excitations at relatively high energies - corresponding to short-wavelength localized excitations. Increasing further the QP potential to largely exceed the Mott gap ($V = 20J = 2U$ in Fig. 9(b)), the spectrum appears as composed of two parts: a low-energy part, associated with regions exhibiting locally incommensurate densities, and hence a similar behavior to that of the incommensurately filled lattice; and a higher-energy part with $\omega \sim U$, associated with localized particle-hole excitations appearing in regions with local Mott behavior at commensurate filling. A similar separation emerges

with the RB distribution as we will see in the following section. As an intermediate conclusion, one can keep in mind that the typical signature of the localization due to the QP potential is best observed when the spectrum possesses subbands and is very broad in k . The spectra for $U = 2J$, $V = 10J$, *e.g.*, displays nicely this fingerprint.

4.3.2. Comparison with random box disorder We now compare the effect of a QP potential seen in the previous section with the effect of true disorder, represented by the RB distribution. We show results for a RB potential having the exact same values of the strength V as those discussed for the QP potential. As already discussed in Ref. [43], the Fourier transform of single-particle excitations for a RB potential differs significantly from those for a QP potential. In particular the gaps occurring for a QP potential are absent for a RB potential, and momentum broadening due to localization occurs at an infinitesimal strength of the RB potential, while a weak QP potential rather leads to excitations with narrow momentum features, and with a quasi-period imposed by the pseudo-Brillouin zone of the QP potential. This is due to the fact that a RB potential scatters Bloch waves at any wave vector, while a (weak) QP potential primarily affects Bloch waves with a wave vector $k \approx k_{\text{QP}}/2, \pi \pm k_{\text{QP}}/2$, etc. On the contrary, a strong QP potential induces a stronger localization than the RB, leading to very broad momentum features. These differences between the RB case and the QP one will clearly persist in the Bogolyubov and HCB regimes. In what follows we check that similar differences are also present for interaction strengths interpolating between the weakly and strongly interacting regimes.

The results for $S(k, \omega)$ in the presence of a RB potential are plotted in Fig. 10. The values for the interaction and disorder strengths are the same as in Fig 9. To avoid repetitions with respect to the discussion of the QP case, we simply highlight the main analogies and differences between the RB and QP case. For the incommensurate density $n = 0.5$ and weak interaction $U = 2J$, we generally observe that an arc-like shape of the $S(k, \omega)$ support, typical of the Bogolyubov mode in the clean case, is preserved in the presence of disorder, but the energy and momentum structure is strongly broadened, due to localization of the modes and to the random distribution of energies of localized excitations induced by disorder. This is in sharp contrast with the subband formation seen in the QP potential. The doublon excitation undergoes a similar fate as for the QP potential, merging rapidly with the acoustic modes for a large enough RB potential. For a stronger repulsion $U = 10J$ the evolution of $S(k, \omega)$ with increasing disorder is comparable to the quasi-periodic case, certainly due to the fact that finite-size effects make the small differences hardly visible. Yet, in the large disorder limit, the spectrum is quite different from the QP, with the absence of subbands and a weight broadly distributed in frequency. In both cases, the spectral weight tends to decrease with V .

Turning to the commensurate case $n = 1$ at weak interaction $U = 2J$, we find that the spectra at weak disorder are comparable to the QP ones, the disorder leading just to broadening of the dispersion, while the spectra at strong RB disorder are remarkably different from the QP case, illustrating the different localization mechanism in the two

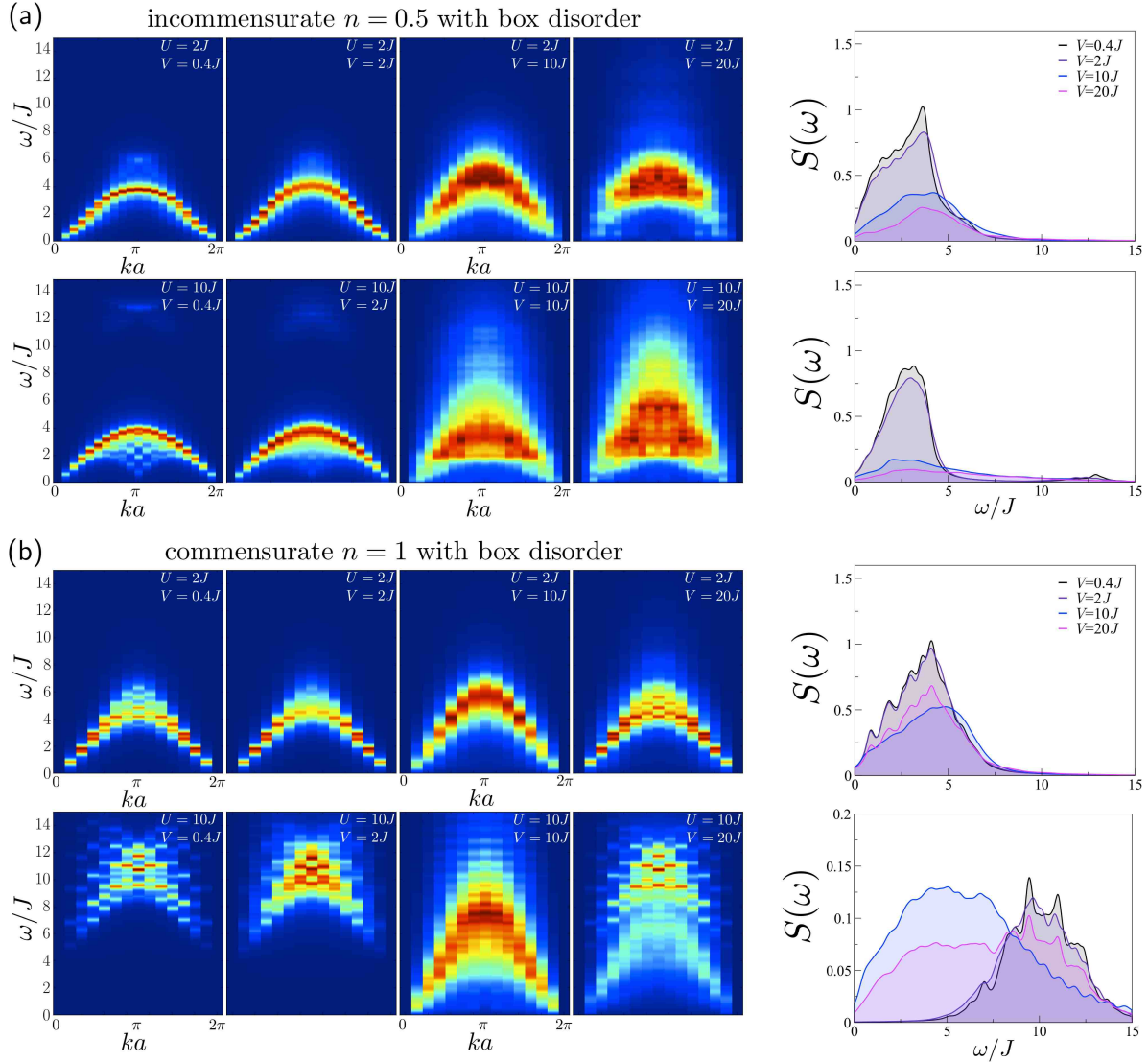


Figure 10. Dynamic density structure factor for the RB disordered system. (a) for a typical incommensurate density $n = 0.5$ ($L = 20$). (b) for the commensurate density $n = 1$ ($L = 14$).

cases. In the case of strong interactions, $U = 10J$, we observe that the RB potential leads to a closing of the Mott gap, similarly to the QP potential, but deep in the Bose-glass phase ($V = 20J$), $S(k, \omega)$ exhibits a rather special structure with two coexisting features: a low-energy arc-shaped part, quantitatively consistent with the incommensurate filling case at the same disorder strength (compare the picture at $U = 2J$), and a high-energy part with the same structure as the particle-hole excitations of the Mott insulator at weak disorder (compare the case $V = 0.4J$). As for the QP potential, this is a clear signature of the strongly-correlated Bose glass regime, with the coexistence of regions with locally incommensurate filling and gapless excitations, and regions which preserve a commensurate filling and a Mott-like behavior – as also seen (albeit less clearly) in the case of the QP potential for the same interaction and potential strength.

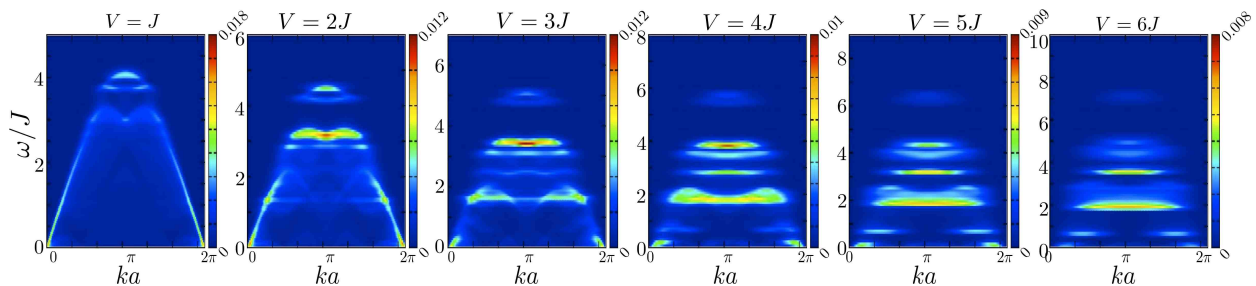


Figure 11. Dynamic structure factor of 1D bosons in a QP potential with variable strength and in a confining parabolic potential with strength $V_i = 10^{-3}J$. Here the QP potential is increased adiabatically at fixed entropy per particle $\mathcal{S}/N = 1 k_B$.

An important conclusion of this section is that, the comparison between QP and RB results at strong disorder shows that Bragg spectroscopy could certainly probe the very nature of the Bose glass phase and unveil the localization mechanism at play.

5. Experimental considerations: finite entropy and ω -scan overlaps

In the previous section we have seen that low-energy features of the spectral function at large U reproduce the HCB behavior. Therefore, one can exploit the exact solution available for the HCB case to make further contact with an experimentally realistic situation. Given that in experiments the loading of the optical lattices occurs in a (quasi)-adiabatic way, we study the evolution of the dynamic structure factor with an increasing height of the secondary lattice at fixed entropy per particle, taken to be $\mathcal{S}/N = 1 k_B$. The corresponding temperature which enters in the calculation of the dynamic structure factor in Eq. (20) is obtained by numerical inversion of the equation which links temperature and entropy for free fermions

$$\mathcal{S}(T) = -k_B \sum_{\alpha} [f_{\alpha} \log f_{\alpha} + (1 - f_{\alpha}) \log(1 - f_{\alpha})] \quad (26)$$

where $f_{\alpha} = f(e_{\alpha}, T)$. In the present case, since the QP potential reduces the density of states at low energy and fragments the energy spectrum into increasingly spaced minibands, entropy conservation implies adiabatic heating of the system as V increases. Yet, the comparison between Figs. 8 and 11 shows that the main features of the localization transition remain intact, indicating that they are accessible to current experiments.

As a second aspect with direct experimental relevance, we propose an effective, global way to capture the dispersive or non-dispersive (namely k -dependent or k -independent) nature of the dynamic structure factor. This amounts to considering

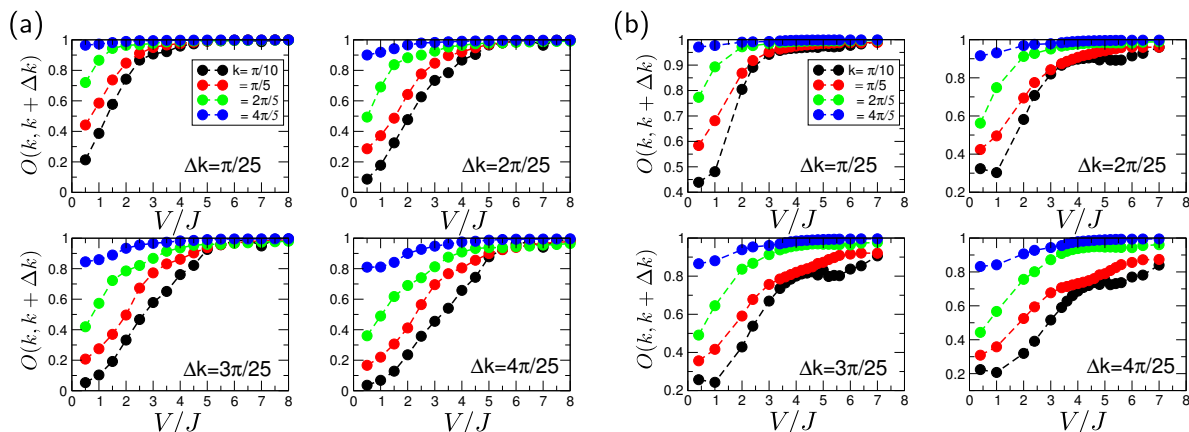


Figure 12. (a) Overlap function of ω -scans in the dynamic structure factor for $N = 60$ hardcore bosons at $T = 0$ and in a QP potential plus a confining parabolic potential. Each panel shows the overlap at four different reference wave vectors k , with an increasing separation Δk when going from the upper-left to the lower-right panel. (b) Same but for finite entropy, $S/N = 1 k_B$.

the *overlap* function of two ω -scans in $S(k, \omega)$ at wave vectors k and $k + \Delta k$:

$$O(k, k + \Delta k) = \frac{\int d\omega S(k, \omega) S(k + \Delta k, \omega)}{\left[\int d\omega S^2(k, \omega) \int d\omega S^2(k + \Delta k, \omega) \right]^{1/2}}. \quad (27)$$

This expression is normalized so that $O(k, k) = 1$, and in general $O(k, k + \Delta k)$ is close to 1 if the features in $S(k, \omega)$ at k and $k + \Delta k$ have a large overlap; if on the other hand $S(k, \omega)$ has strongly dispersive features, O is in general $\ll 1$ - it exactly vanishes in the extreme limit of a $S(k, \omega) \sim \delta(\omega - \epsilon_k)$, displaying a δ -ridge associated with a dispersion relation ϵ_k having a finite group velocity around k , $d\epsilon_k/dk \neq 0$.

In Figs. 12(a-b) we show the overlap function at zero and finite entropy ($1 k_B$ per particle) respectively, for four different values of k (going from the Brillouin zone center towards the edge) and for four values of the separation Δk between ω -scans, as a function of the QP potential strength V . For all scans we observe that the overlap increases for $V/J \rightarrow 4^-$, and it displays plateaus in the localized phase; this feature is not only robust to the presence of a confining potential, but also to the presence of a finite entropy. In particular we observe that the overlap is most sensitive to the localization transition when k is close to the zone center, because this is the wave-vector region in which the features in $S(k, \omega)$ display the strongest k dependence in the delocalized phase. Unsurprisingly, the sharpest features in O at the localization transition are displayed for the largest Δk separation we investigated. Therefore the overlap provides a quantitative estimate of the localization transition based on the dynamic structure factor. Its effectiveness relies upon the fact that, in the problem at hand, *all* excitation modes localize and lose their dispersive nature at the ground-state transition point $V = 4J$. Yet it can be extended to situations (as the one discussed

in Section 4.1) in which only a part of the excited states in the excitation spectrum localizes. Most importantly, the overlap is a convenient experimental observable which allows to detect the transition even when one does not have access experimentally to the whole (k, ω) plane. Indeed several recent experiments [64, 36, 39, 40] have measured ω -scans for a fixed k or a small range of k values (limited by the optical access to the sample). We observe that the overlap is well adapted to such a situation, providing a direct inspection into the localization transition by using only two tomographic scans of the dynamic structure factor at near wave-vectors.

6. Summary and conclusions

In conclusion, we have shown that the study of the dynamic structure factor provides important information on the interplay of disorder and interactions in one dimensional Bose fluids. Our analysis relies upon exact diagonalization results at arbitrary interactions, Bogolyubov theory for the weakly interacting case, and the exact solution for the hardcore case. Already in the clean case, the dynamic structure factor displays different features in the various interaction regimes, from sharp dispersive features in the weakly interacting superfluid phase, to a broad particle-hole continuum in the strongly-interacting (but still superfluid) phase, coexisting with a doublon mode. Once the disorder is turned on, we have shown that the dynamic structure factor allows to explore the spatial support of the excitations, yielding information on their localization properties. We have also investigated the features of the dynamic structure factor in the presence of a random-box disorder, from weak to strong interactions, showing that the dynamic structure factor captures the differences in the spectral features of the excitations with respect to the quasi-periodic potential. Thereby, it can probe in a direct way the localization mechanism. Finally, by exploiting the exact solution available for the hardcore-boson limit, we have shown that the main features of localization exhibited by the dynamic structure factor at zero temperature remain visible at a realistic finite entropy; and we have suggested an experimentally viable method to extract information on the Bose-glass transition at strong interactions, by analyzing frequency scans in the dynamic structure factor at two fixed and near wave vectors. While our paper exclusively focuses on the one-dimensional case, we argue that the insight provided by the dynamic structure factor into the physics of disordered bosons will be extremely useful also in higher-dimensional cases. In particular, the sensitivity of the dynamic structure factor to the extended or localized nature of the excitation modes, in a given frequency range, makes it a most viable probe of the presence of a mobility edge in the spectrum, which is a characteristic feature of higher-dimensional systems [5, 6].

6.1. Acknowledgments

Useful discussions with N. Fabbri, L. Fallani, C. Fort, and E. Orignac are gratefully acknowledged. GR acknowledges support from the Agence Nationale de la Recherche

under grant ANR-2011-BS040-012-01 QuDec and AM from the ERC grant "Handy-Q" No. 258608. Numerical calculations were partially performed on the computer cluster of the PSMN (ENS Lyon).

References

- [1] L. Sanchez-Palencia and M. Lewenstein, *Nature Physics* **6**, 87 (2010).
- [2] J. Billy *et al.*, *Nature* **453**, 891 (2008).
- [3] M. Pasienski *et al.*, *Nat. Phys.* **6**, 677 (2010).
- [4] M. Robert-de Saint-Vincent *et al.*, *Phys. Rev. Lett.* **104**, 220602 (2010).
- [5] S. S. Kondov, W. R. McGehee, J. Zirbel, and B. DeMarco, *Science* **334**, 66 (2011).
- [6] F. Jendrzejewski *et al.*, *Nature Physics* **8**, 398 (2012).
- [7] F. Jendrzejewski *et al.*, *Phys. Rev. Lett.* **109**, 195302 (2012).
- [8] L. Fallani *et al.*, *Phys. Rev. Lett.* **98**, 130404 (2007).
- [9] J. E. Lye *et al.*, *Phys. Rev. A* **75**, 061603 (2007).
- [10] V. Guarrera *et al.*, *New J. Phys.* **9**, 107 (2007).
- [11] V. Guarrera *et al.*, *Phys. Rev. Lett.* **100**, 250403 (2008).
- [12] G. Roati *et al.*, *Nature* **453**, 895 (2008).
- [13] B. Deissler *et al.*, *Nat. Phys.* **6**, 354 (2010).
- [14] B. Deissler *et al.*, *New Journal of Physics* **13**, 023020 (2011).
- [15] E. Lucioni *et al.*, *Phys. Rev. Lett.* **106**, 230403 (2011).
- [16] S. Aubry and G. André, *Ann. Israel. Phys. Soc.* **3**, 133 (1980).
- [17] T. Giamarchi and H. J. Schulz, *Europhys. Lett.* **3**, 1287 (1987).
- [18] T. Giamarchi and H. J. Schulz, *Phys. Rev. B* **37**, 325 (1988).
- [19] M. P. A. Fisher, P. B. Weichman, G. Grinstein, and D. S. Fisher, *Phys. Rev. B* **40**, 546 (1989).
- [20] R. Ozeri, N. Katz, J. Steinhauer, and N. Davidson, *Rev. Mod. Phys.* **77**, 187 (2005).
- [21] C. Menotti, M. Krämer, L. Pitaevskii, and S. Stringari, *Phys. Rev. A* **67**, 053609 (2003).
- [22] J.-S. Caux and P. Calabrese, *Phys. Rev. A* **74**, 031605 (2006).
- [23] J.-S. Caux, P. Calabrese, and N. A. Slavnov, *J. Stat. Mech.* **2007**, P01008 (2007).
- [24] P. Calabrese and J.-S. Caux, *Phys. Rev. Lett.* **98**, 150403 (2007).
- [25] E. Orignac, R. Citro, S. De Palo, and M.-L. Chiofalo, *Phys. Rev. A* **85**, 013634 (2012).
- [26] S. D. Huber, E. Altman, H. P. Büchler, and G. Blatter, *Phys. Rev. B* **75**, 085106 (2007).
- [27] V. N. Golovach, A. Minguzzi, and L. I. Glazman, *Phys. Rev. A* **80**, 043611 (2009).
- [28] T. D. Graß, F. E. A. dos Santos, and A. Pelster, *Phys. Rev. A* **84**, 013613 (2011).
- [29] R. Roth and K. Burnett, *J. Phys. B: At. Mol. Opt. Phys.* **37**, 3893 (2004).
- [30] G. G. Batrouni, F. F. Assaad, R. T. Scalettar, and P. J. H. Denteneer, *Phys. Rev. A* **72**, 031601 (2005).
- [31] A. M. Rey *et al.*, *Phys. Rev. A* **72**, 023407 (2005).
- [32] G. Pupillo, A. M. Rey, and G. G. Batrouni, *Phys. Rev. A* **74**, 013601 (2006).
- [33] P. Pippan, H. G. Evertz, and M. Hohenadler, *Phys. Rev. A* **80**, 033612 (2009).
- [34] S. Ejima, H. Fehske, and F. Gebhard, *Europhys. Lett.* **93**, 30002 (2011).
- [35] S. Ejima *et al.*, *Phys. Rev. A* **85**, 053644 (2012).
- [36] D. Clément *et al.*, *Phys. Rev. Lett.* **102**, 155301 (2009).
- [37] X. Du *et al.*, *New Journal of Physics* **12**, 083025 (2010).
- [38] P. Ernst *et al.*, *Nature Physics* **6**, 56 (2010).
- [39] N. Fabbri *et al.*, *Phys. Rev. A* **83**, 031604 (2011).
- [40] N. Fabbri *et al.*, *Phys. Rev. Lett.* **109**, 055301 (2012).
- [41] G. Orso, A. Iucci, M. A. Cazalilla, and T. Giamarchi, *Phys. Rev. A* **80**, 033625 (2009).
- [42] M. Knap, E. Arrigoni, and W. von der Linden, *Phys. Rev. A* **82**, 053628 (2010).
- [43] G. Roux *et al.*, *Phys. Rev. A* **78**, 023628 (2008).

- [44] G. G. Batrouni, R. T. Scalettar, and G. T. Zimanyi, *Phys. Rev. Lett.* **65**, 1765 (1990).
- [45] R. T. Scalettar, G. G. Batrouni, and G. T. Zimanyi, *Phys. Rev. Lett.* **66**, 3144 (1991).
- [46] J. K. Freericks and H. Monien, *Phys. Rev. B* **53**, 2691 (1996).
- [47] N. V. Prokof'ev and B. V. Svistunov, *Phys. Rev. Lett.* **80**, 4355 (1998).
- [48] S. Rapsch, U. Schollwöck, and W. Zwerger, *Europhys. Lett.* **46**, 559 (1999).
- [49] B. Simon, *Advances in Applied Mathematics* **3**, 463 (1982).
- [50] J. Sokoloff, *Phys. Rep.* **126**, 189 (1985).
- [51] D. J. Thouless, *Phys. Rev. B* **28**, 4272 (1983).
- [52] M. Kohmoto, L. P. Kadanoff, and C. Tang, *Phys. Rev. Lett.* **50**, 1870 (1983).
- [53] C. Tang and M. Kohmoto, *Phys. Rev. B* **34**, 2041 (1986).
- [54] H. Hiramoto and M. Kohmoto, *Int. J. Mod. Phys. B* **06**, 281 (1992).
- [55] D. Barache and J. M. Luck, *Phys. Rev. B* **49**, 15004 (1994).
- [56] M. Albert and P. Leboeuf, *Phys. Rev. A* **81**, 013614 (2010).
- [57] J. Vidal, D. Mouhanna, and T. Giamarchi, *Phys. Rev. Lett.* **83**, 3908 (1999).
- [58] J. Vidal, D. Mouhanna, and T. Giamarchi, *Phys. Rev. B* **65**, 014201 (2001).
- [59] R. Roth and K. Burnett, *Phys. Rev. A* **68**, 023604 (2003).
- [60] T. Roscilde, *Phys. Rev. A* **77**, 063605 (2008).
- [61] X. Deng, R. Citro, A. Minguzzi, and E. Orignac, *Phys. Rev. A* **78**, 013625 (2008).
- [62] D. Pines and P. Nozieres, *The theory of quantum liquids* (W.A. Benjamin, New York, 1966).
- [63] A. Brunello *et al.*, *Phys. Rev. A* **64**, 063614 (2001).
- [64] G. Veeravalli, E. Kuhnle, P. Dyke, and C. J. Vale, *Phys. Rev. Lett.* **101**, 250403 (2008).
- [65] B. Lu *et al.*, *Phys. Rev. A* **83**, 051608 (2011).
- [66] C. Mora and Y. Castin, *Phys. Rev. A* **67**, 053615 (2003).
- [67] J.-P. Blaizot and G. Ripka, *Quantum Theory of Finite Systems* (MIT Press, Cambridge, MA (USA), 1986).
- [68] L. Fontanesi, M. Wouters, and V. Savona, *Phys. Rev. Lett.* **103**, 030403 (2009).
- [69] L. Fontanesi, M. Wouters, and V. Savona, *Phys. Rev. A* **81**, 053603 (2010).
- [70] P. Lugan and L. Sanchez-Palencia, *Phys. Rev. A* **84**, 013612 (2011).
- [71] C. Gaul and C. A. Müller, *Phys. Rev. A* **83**, 063629 (2011).
- [72] L. Fontanesi, *PhD Thesis, EPFL* (unpublished, Lausanne, 2011).
- [73] W.-C. Wu and A. Griffin, *Phys. Rev. A* **54**, 4204 (1996).
- [74] F. Zambelli, L. Pitaevskii, D. M. Stamper-Kurn, and S. Stringari, *Phys. Rev. A* **61**, 063608 (2000).
- [75] E. V. Castro, N. M. R. Peres, K. S. D. Beach, and A. W. Sandvik, *Phys. Rev. B* **73**, 054422 (2006).
- [76] E. Lieb, T. Schultz, and D. Mattis, *Ann. Phys.* **16**, 407 (1961).
- [77] K. Winkler *et al.*, *Nature* **441**, 853 (2006).
- [78] A. Imambekov, T. Schmidt, and L. Glazman, *Rev. Mod. Phys.* **84**, 1253 (2012).
- [79] J. des Cloizeaux and J. J. Pearson, *Phys. Rev.* **128**, 2131 (1962).
- [80] C. Mora and Y. Castin, *Phys. Rev. A* **67**, 053615 (2003).
- [81] A. Cetoli and E. Lundh, *Phys. Rev. A* **81**, 063635 (2010).
- [82] C. Gaul, N. Renner, and C. A. Müller, *Phys. Rev. A* **80**, 053620 (2009).
- [83] C. Gaul and C. A. Müller, *Phys. Rev. A* **83**, 063629 (2011).